

Do tunneling states and boson peak persist or disappear in extremely stabilized glasses?

M.A. Ramos and T. Pérez-Castañeda

*Laboratorio de Bajas Temperaturas, Departamento de Física de la Materia Condensada
Condensed Matter Physics Center (IFIMAC) and Instituto de Ciencia de Materiales “Nicolás Cabrera”
Universidad Autónoma de Madrid, Cantoblanco, Madrid E-28049, Spain
E-mail: miguel.ramos@uam.es*

R.J. Jiménez-Riobóo

Instituto de Ciencia de Materiales de Madrid (ICMM-CSIC), Cantoblanco, Madrid E-28049, Spain

C. Rodríguez-Tinoco and J. Rodríguez-Viejo

*Nanomaterials and Microsystems Group, Physics Department, and MATGAS Research Centre
Universitat Autònoma de Barcelona, Bellaterra E-08193, Barcelona, Spain*

Received September 4, 2014, published online April 23, 2015

We review and concurrently discuss two recent works conducted by us, which apparently give opposite results. Specifically, we have investigated how extreme thermal histories in glasses can affect their universal properties at low temperatures, by studying: (i) amber, the fossilized natural resin, which is a glass which has experienced a hyperaging process for about one hundred million years; and (ii) ultrastable thin-film glasses of indomethacin. Specific heat C_p measurements in the temperature range $0.07 \text{ K} < T < 30 \text{ K}$ showed that the amount of two-level systems, assessed from the linear term at the lowest temperatures, was exactly the same for the pristine hyperaged amber glass as for the subsequently rejuvenated samples, whereas just a modest increase of the boson-peak height (in C_p/T^3) with increasing rejuvenation was observed, related to a corresponding increase of the Debye coefficient. On the other hand, we have observed an unexpected suppression of the two-level systems in the ultrastable glass of indomethacin, whereas conventionally prepared thin films of the same material exhibit the usual linear term in the specific heat below 1 K ascribed to these universal two-level systems in glasses. By comparing both highly-stable kinds of glass, we conclude that the disappearance of the tunneling two-level systems in ultrastable thin films of indomethacin may be due to the quasi-2D and anisotropic behavior of this glass, what could support the idea of a phonon-mediated interaction between two-level systems.

PACS: **65.60.+a** Thermal properties of amorphous solids and glasses: heat capacity, thermal expansion, etc.;
64.70.P– Glass transitions of specific systems;
63.50.Lm Glasses and amorphous solids;
81.40.Cd Solid solution hardening, precipitation hardening, and dispersion hardening; aging.

Keywords: low-temperature thermal properties of glasses; specific heat; glass transition; tunneling two-level systems; ultrastable glasses

1. Introduction

Glasses and amorphous solids, in general, and even some disordered crystalline solids, exhibit thermal and acoustic properties at low temperatures anomalously different from those found in crystalline solids [1,2]. Furthermore, these low-temperature glassy properties show a

remarkable degree of universality for any glass, irrespective of the type of material, chemical bonding, etc. Hence the low-temperature properties of noncrystalline solids are said to exhibit a universal “glassy behavior”. In particular, below about 1 K the specific heat of glasses depends quasilinearly on temperature, $C_p \propto T^{1+\delta}$, and the thermal conductivity almost quadratically, $\kappa \propto T^{2-\delta}$, in clear con-

trast with the cubic dependences successfully predicted by Debye theory for crystals. On the other hand, the thermal behavior of glasses above 1 K and their corresponding low-frequency vibrational properties around 1 THz, are dominated by another universal but most controversial feature of glasses: the so-called “boson peak” [2,3] arising from a noteworthy excess in the vibrational density of states (VDOS) over that predicted by Debye’s theory $g(\omega) \propto \omega^2$. Such an excess in the low-frequency VDOS appears as a broad peak in $g(\omega)/\omega^2$, which produces a corresponding broad maximum in C_p/T^3 , observed in glasses at typically 3–10 K [2].

The formerly mentioned thermal properties of glasses below 1 K, as well as related acoustic and dielectric properties of amorphous solids at low temperatures [2], were since long successfully accounted for [4,5] by the Tunneling Model (TM). The core idea of the TM is the ubiquitous existence of atoms or groups of atoms in amorphous solids due to the intrinsic atomic disorder, which can perform quantum tunneling between two configurations of very similar energy, usually named tunneling states or two-level systems (TLS). Nevertheless, a very few authors [6,7] raised later strong criticisms against the standard TM, pointing out how improbable was that a random ensemble of independent tunneling states would produce essentially the same universal constant for the thermal conductivity or the acoustic attenuation in any substance. Most experimentalists, however, have continued to trust the TM, given its both simplicity and apparent success to account for the experimental data. As said above, the thermal properties of glasses above 1 K and their low-frequency vibrational spectrum dominated by the boson peak at 1 THz, are still much more controversial and poorly understood [3].

In this article we present and discuss together two recent experimental works [8,9] conducted by us, aimed at investigating whether this universal behavior of glasses persists or not in glasses subjected to unusually strong processes of thermodynamic and kinetic stabilization. Specifically, we have studied two very different kinds of *extremely stable* glasses. First, we have measured the specific heat of 110 million-year-old amber samples from the cave of El Soplao (Spain), both at very low temperatures and around the glass transition T_g [8]. Amber is essentially a fossilized tree resin that polymerized millions of years ago. Of interest here, amber is a unique example of a (polymer) glass that has aged far longer than any system accessible in the laboratory, thus reaching a state (of lower enthalpy and entropy) which is not accessible under normal experimental conditions. In other words, it is an amorphous solid or glass which has experienced an extreme thermodynamic stabilization process (*hyperageing*) [10]. Second, we have also studied the specific heat of *ultrastable glasses* of indomethacin [9]. So-called ultrastable glasses, showing unprecedented thermodynamic and kinetic stability, have

recently been synthesized by physical vapor-deposition of several organic molecules in short-time scales [11–16]. An appropriate deposition rate in combination with an optimal substrate temperature (typically around $0.85 T_g$) have proved to drastically favour two-dimensional mobility and, as a consequence, access to local minima of very low energy in the potential-energy landscape [17,18]. An ordinary glass obtained by supercooling the liquid should theoretically be aged for 10^3 – 10^9 years in order to achieve the same stability and density of these vapor-deposited glasses [19].

Interestingly, we have found clear-cut but opposite results in the two cases. Although this makes it more difficult to draw a simple conclusion, it certainly provides us with complementary information to shed light on the long-standing mystery of the nature of low-energy excitations in glasses, responsible for the universal glassy behavior at low temperatures.

2. Experimental techniques

The samples of amber used in these experiments [8] were obtained from a new amber deposit discovered quite recently in the northern region of Spain, in Cantabria, within El Soplao territory [20], and have been dated to be 110–112 million years old. When necessary, raw pieces of amber were cleaved or slowly cut with a diamond wheel, and then simply cleaned with distilled water. After being completely measured and characterized, some pristine samples of amber were either partially or totally rejuvenated, by means of an isothermal annealing process at $T_g = 423$ K during 2 hours or by heating the sample well above T_g followed by cooling at 1 K/min, respectively [8]. Other different thermal treatments conducted to study in detail the calorimetry and thermodynamics around the glass transition can also be seen in [8]. The Debye contribution to the specific heat was independently determined for the three samples studied at low temperatures from the experimental values of the sound velocity and mass density. The longitudinal sound velocity was measured in the temperature range $80 \text{ K} \leq T \leq 300 \text{ K}$ using High Resolution Brillouin Spectroscopy (HRBS), with excitation wavelength $\lambda_0 = 514.5$ nm, and extrapolated to 0 K with a least-squares fit, as shown in Fig. 1 and in Table 1. Polished plan-parallel slabs of amber, less than 0.5 mm thick were employed. Both backscattering (180°) and right-angle (90° A) geometries were simultaneously used, the former implying a refractive-index dependent acoustic wave vector and the latter being independent of it. Given the high background signal introduced by the luminescence of the samples at these wavelengths, the transverse sound velocities v_T could not be measured by HRBS. However, the zero-temperature values $v_T(0)$ could be approximately obtained by means of the generalized Cauchy equation [8,21], and are also

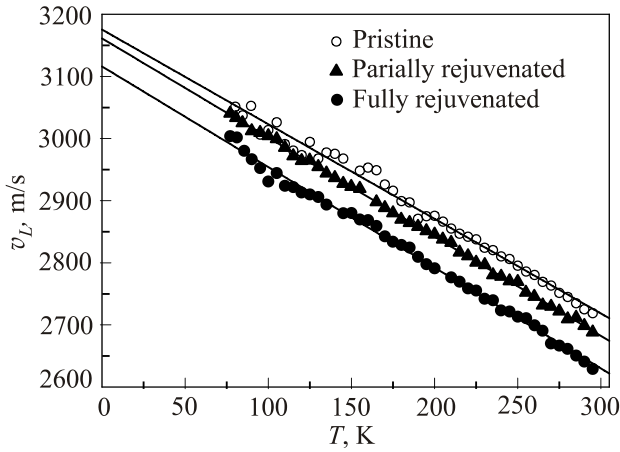


Fig. 1. Temperature dependence of the longitudinal sound velocities in amber from El Soplao with decreasing stability, measured by High Resolution Brillouin Spectroscopy. Least-squares fits of the experimental data in the temperature range $80 \text{ K} \leq T \leq 300 \text{ K}$ are used to calculate the zero-temperature extrapolation $v_L^{\text{prs}}(0 \text{ K}) = 3175 \text{ m/s}$, $v_L^{\text{ann}}(0 \text{ K}) = 3160 \text{ m/s}$ and $v_L^{\text{rej}}(0 \text{ K}) = 3115 \text{ m/s}$, for the pristine, annealed (= partially rejuvenated) and fully rejuvenated samples, respectively.

displayed in Table 1. The mass density of the three samples was measured at room temperature by means of the Archimedes method with a Mettler Toledo AB 265-S balance, using distilled water as a fluid. Linear extrapolation of the mass densities to zero temperature were done by recourse to the Lorenz–Lorentz relation between mass density $\rho(T)$ and refractive index $n(T)$ for a transparent medium, after our HRBS measurements as a function of temperature in the range $80 \text{ K} < T < 300 \text{ K}$.

Indomethacin ($\text{C}_{19}\text{H}_{16}\text{ClNO}_4$, $T_g = 315 \text{ K}$, $T_m = 428 \text{ K}$) crystalline powders with 99% purity were purchased from Sigma–Aldrich. The fabrication of the ultrastable glass of indomethacin (IMC) [9] was done under ultrahigh-vacuum conditions $P < 10^{-8}$ mbar, by vapor-depositing the organic molecule onto a silicon substrate kept isothermally at temperature $T_{\text{subs}} = 0.85 \cdot T_g = 266 \text{ K}$. The deposition rate for the samples presented here was kept constant at $\sim 0.1 \text{ nm/s}$,

which was observed to produce samples with optimal stability. The growth rate was $(0.15 \pm 0.05) \text{ nm/s}$. The thickness of the films ranged from 50 to 80 μm , in order to enhance the signal-to-noise ratio in the low- T specific-heat measurements. All samples were stored in vacuum-sealed bags with desiccant in a freezer to minimize aging prior to the low- T specific heat measurements. Low-temperature data of the ultrastable glasses in high vacuum was acquired few days after preparation, with the exception of a sample stored in those conditions for two months, named “degraded” ultrastable glass. We also carried out x-ray diffraction (XRD) measurements using an X’Pert diffractometer from Phillips in the Bragg–Brentano configuration with $\text{Cu K}\alpha$ radiation, in order to confirm the glassy nature of the as-grown samples. The samples were scanned in Bragg–Brentano geometry from $2\theta = 2^\circ$ to 300° with an angular step of 0.025° (0.05°) and time per point of 18 (12) s for the ultrastable and conventional IMC glasses, respectively. We also conducted experiments at the beamline ID28 of the European Synchrotron Radiation Facility (ESRF), with the energy of the x rays set to 23.725 eV. Photons were detected with a photodiode with the sample aligned parallel (in-plane) or perpendicular (out-of-plane) to the detector axis (see Fig. 3 of Ref. 9).

Calorimetric characterization of amber through the different stages of rejuvenation (thermodynamic destabilization) was performed using a commercial DSC Q100 from TA Instruments. The technique employed was temperature-modulated differential scanning calorimetry (TM-DSC), which allowed us to independently determine thermodynamic and kinetic stability via reversing and non-reversing contributions to the heat capacity, as well as the total heat capacity [8]. Heating and cooling rates employed were always $\pm 1 \text{ K/min}$, and modulating signals $\pm 0.5 \text{ K}$ every 80 s. To characterize the calorimetric behavior of different glasses and crystals of IMC, a DSC Perkin Elmer 7 was used with heating scans at a rate of 10 K/min on IMC thin films with masses of the order of 8–11 mg. Whereas the first scan usually corresponds to an ultrastable glass, the second upscan is characteristic of a conventional glass obtained by cooling the liquid at 10 K/min.

Table 1. Calorimetric data for amber: Glass-transition temperatures T_g^* and fictive temperatures T_f obtained after the different thermal histories applied to the studied samples. $(T_f - T_f^0)/T_f^0$ displays the relative decrease of the fictive temperature T_f in relation to the canonical reference glass obtained after fully rejuvenation and cooling at 10 K/min. Elastic data: measured mass density at room temperature ρ_{RT} and zero-temperature extrapolated $\rho(0)$, longitudinal $v_L(0)$ and transverse $v_T(0)$ sound velocity, average Debye velocity in the zero-temperature limit v_D and correspondingly calculated cubic Debye coefficient c_D for the specific heat.

Sample State	T_g^* , K	T_f , K	$(T_f - T_f^0)/T_f^0$	ρ_{RT} , kg/m^3	$\rho(0)$, kg/m^3	$v_L(0)$, m/s	$v_T(0)$, m/s	v_D , m/s	c_D , $\mu\text{J}\cdot\text{g}^{-1}\cdot\text{K}^{-4}$
Pristine (hyperaged)	438	384	-7.7%	1045	1055	3175	1635	1831	18.9
Partially rejuvenated	436	391	-6.0%	1038	1049	3160	1625	1820	19.3
Fully rejuvenated (canonical glass)	423	416	0%	1024	1035	3115	1596	1788	20.7

In all cases, the low-temperature specific heat in the temperature range from 0.07 K to 30 K was measured by means of thermal relaxation calorimetry [20]. Low-temperature specific-heat measurements in the range $1.8 \text{ K} < T < 30 \text{ K}$ were performed in a double-chamber insert, placed in a ^4He cryostat. Measurements in the range $0.07 \text{ K} < T < 3 \text{ K}$ were performed in a dilution refrigerator Oxford Instruments MX400. In the case of amber samples, calorimetric cells consisted of a sapphire disc, on which a small calibrated thermometer (either Cernox or RuO_2 , respectively) and a resistive chip as a Joule heater were glued diametrically opposed using cryogenic varnish GE7301. The sapphire substrate is suspended from a copper ring acting as thermally-controlled sink. In the case of IMC samples, those used for the low-temperature specific-heat measurements were all grown on silicon substrates of dimension $12 \times 12 \text{ mm}$, and with typical masses $m \approx 0.1 \text{ g}$, what enabled us the handling of the samples, as well as optimal attachment and thermal contact to the calorimetric cell. The main thermal contact between the calorimetric cell and the thermal bath is a thin metallic wire through which heat is released. The heat capacity of the empty addenda was independently measured in each case and subtracted from the total data points. Excellent agreement was found between experimental data from both experimental setups in the overlapping temperature range.

3. Experimental results

3.1. Amber

The first and most important characterization of the amber samples was to perform DSC experiments to confirm their presumed hyperaging and corresponding thermodynamic stabilization. As can be seen in Fig. 2(a) of Ref. 8, a huge endothermic peak is observed for the pristine amber at the calorimetric glass-transition (strictly speaking, devitrification) temperature $T_g^* = 438 \text{ K}$ (here determined by the inflection point of the reversing C_p jump). T_g^* is well above the genuine glass transition temperature $T_g = 423 \text{ K}$ obtained for the rejuvenated sample, or alternatively from the second or third heating runs for any sample, when the cooling and heating rates are canonically the same. This unusual increase of the calorimetric T_g^* for the stabilized amber compared to the canonical glass (see Table 1) is also observed in the case of ultrastable glasses of IMC, and has been ascribed [11] in ultrastable glasses obtained from physical vapor deposition to a high kinetic stability, indicating that much higher temperatures are needed to dislodge the molecules from their glassy configurations.

From the calorimetric curves, the enthalpy as a function of temperature was obtained by direct integration. It is traditional and useful to determine the so-called fictive temperature T_f , defined as the temperature at which the nonequilibrium (glass) state and its equilibrium (super-

cooled liquid) state would have the same enthalpy. The obtained values of T_f for the pristine, partially rejuvenated and fully rejuvenated samples are displayed in Table 1. The observed extraordinary decrease $\Delta T_f = -32 \text{ K}$ (thermodynamic stability) for the pristine amber compared to the rejuvenated glass is similar or even superior to the effects seen in some ultrastable thin films of organic glasses [11,19,23]. Such an extraordinary reduction $\sim 8\%$ of the fictive temperature due to the extremely long aging of amber is indeed the consequence of extremely prolonged sub-sub- T_g structural relaxations [24].

In Fig. 2, we present our consecutive specific-heat measurements for an amber sample in three different states: pristine, partially-rejuvenated (after annealing at 423 K for 2 h) and fully-rejuvenated. Fig. 2(a) is a log-log plot at the lowest temperatures, which emphasizes that the TLS-dominated specific heat below 1 K, remains invariable within experimental error. On the other hand, above 1 K the specific heat moderately increases with rejuvenation around the “boson peak” in C_p/T^3 , see Fig. 2(b), following the same trend as the elastic Debye coefficient obtained from both Brillouin-scattering sound velocity (Fig. 1) and mass-density measurements (see Table 1). However, the position of the peak remains fixed at $(3.4 \pm 0.1) \text{ K}$ in all cases.

3.2. Indomethacin

We measured the specific heat of the two above-mentioned ultrastable glasses (USG) of $50 \mu\text{m}$ - (USG-1) and $80 \mu\text{m}$ - (USG-2) thin films, grown under slightly different conditions, as well as of a conventionally prepared glass and of the crystalline state (in this case, we measured only above 2 K, since the cubic Debye limit had been already reached, allowing a direct extrapolation to lower temperatures). Finally, also a degraded ultrastable glass, after being stored for two months in poor vacuum conditions, hence absorbing water and losing its ultrastability, was measured. Similarly to the case of amber samples, we display the low-temperature specific heat measurements of different states of IMC in two complementary plots: Fig. 3(a) depicts the whole specific-heat data in the Debye-reduced C_p/T^3 representation, where as Fig. 3(b) amplifies the very-low-temperature region in the usual C_p/T vs T^2

Table 2. Coefficients and statistical errors obtained from least-squares linear fits at low temperatures to the function $C_p = c_{\text{TLS}}T + c_D T^3$ for indomethacin (see Fig. 3)

	$c_{\text{TLS}}, \mu\text{J/g}\cdot\text{K}^2$	$c_D, \mu\text{J/g}\cdot\text{K}^4$
Crystal	–	15.0 ± 0.3
Conventional glass	13.7 ± 0.3	49.4 ± 0.2
Ultrastable glass #1	0.2 ± 0.9	46.4 ± 0.6
Ultrastable glass #2	0.02 ± 0.8	36.9 ± 0.4
Degraded USG	13.0 ± 0.7	40.6 ± 0.5

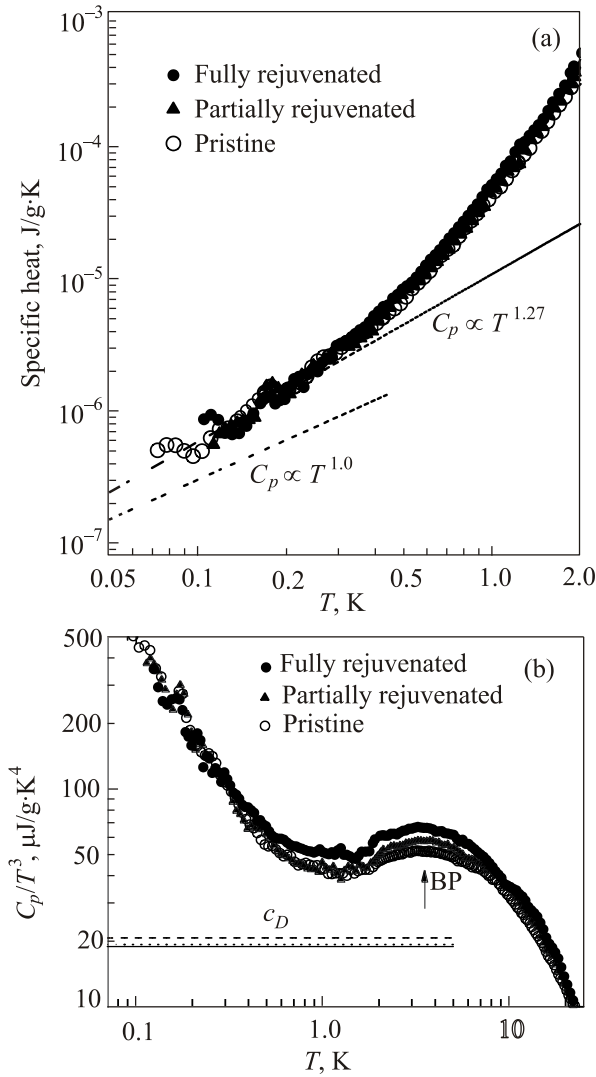


Fig. 2. Specific-heat data for three different states (pristine, partially-rejuvenated and fully-rejuvenated) of the same amber sample at very low temperatures, 0.05–2 K. The upper dashed line shows the best quasilinear fit $C_p \propto T^{1+\delta}$ to the experimental data below 0.4 K given by $C_p \propto T^{1.27}$, hence faster than the simple linear dependence indicated by the lower dashed line (a). C_p/T^3 plot of the same data in (a), displayed in a wider temperature range. The height of the boson peak is observed to further increase with rejuvenation, though the values of both the minimum and the maximum of C_p/T^3 remain constant: $T_{\min} = (1.2 \pm 0.1)$ K and $T_{\max} = (3.4 \pm 0.1)$ K, respectively. The corresponding Debye levels determined from the sound velocity and density data (Table 1) are indicated by solid lines, and exhibit the same trend as the boson-peak height (both sets follow the same order as the symbols in the legend) (b).

plot where a least-squares linear fit provides the TLS linear term (the intercept with the y axis) and the Debye coefficient (the slope). The crystal of indomethacin exhibits the expected $C_p \propto T^3$ below 8 K. The same shoulder-like behavior (a very shallow *boson peak*, as typically occur in other fragile glass formers [25]) is observed in both ultrastable and ordinary glasses below ~ 5 K in Fig. 3(a).

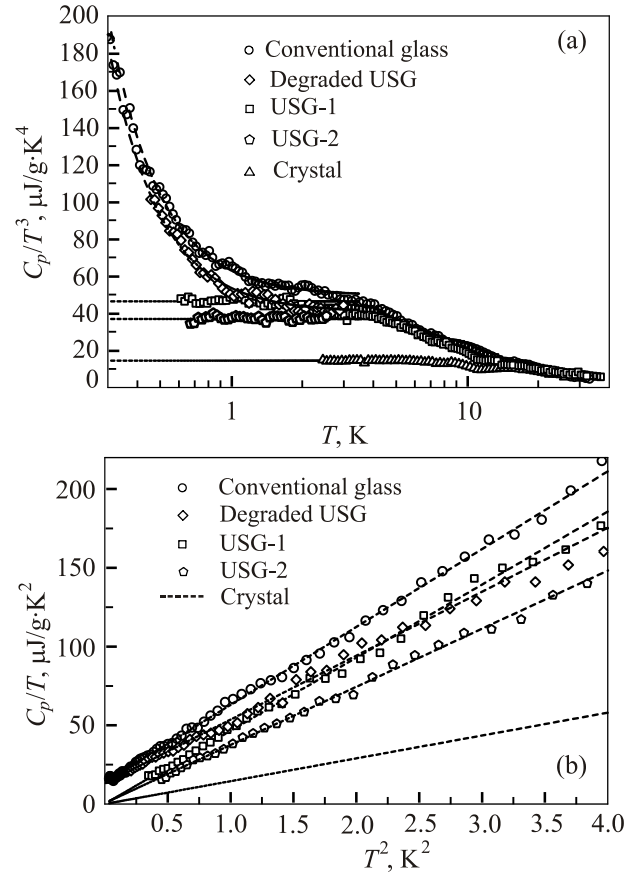


Fig. 3. Low-temperature specific-heat data for two differently prepared ultrastable glasses of indomethacin: 50 μm - (USG-1) and 80 μm - (USG-2) thin films, compared to the crystalline phase (Debye extrapolated at lower temperatures) and the conventional glass. A degraded ultrastable glass (see Experimental techniques) has also been measured and is presented. Dashed lines show the corresponding linear fits $C_p = c_{\text{TLS}}T + c_D T^3$ for experimental data below 2 K. Debye-reduced C_p/T^3 vs T representation (a); C_p/T vs T^2 plot at very low temperatures to determine the TLS and Debye coefficients, which are shown in Table 2 (b).

Nevertheless, the most surprising behavior found in both ultrastable glasses is the full suppression of the linear term of the specific heat ascribed to the tunneling TLS. This is demonstrated in Fig. 3(b), where the intercept with the ordinate axis goes to zero within experimental error (see Table 2), in clear contrast with the case of conventional glass, or even for the degraded ultrastable glass.

4. Discussion

Whether or not the low-temperature universal “anomalies” of glasses (dominated by low-energy excitations not present in crystals, i.e., tunneling TLS and the boson peak) could be eventually suppressed by much stronger and longer annealing or ageing processes, and hence whether they are or not intrinsic properties of the glass state, has been an unsolved question during the last forty years. Indeed, different experiments [26–32] have been reported

about the possible influence of the thermal history on these low-temperature properties, but with contradictory conclusions (see a more detailed discussion on those experiments in Ref. 8). Besides, there have been a few reports [33–36] claiming the absence of TLS in some particular amorphous solids. Angell *et al.* [37] proposed the designation of “superstrong liquids” for some “tetrahedral liquids” which could be potential “perfect glasses”, with a residual entropy near zero, and where the defect-related boson peak and TLS excitations were weak or absent. Specifically, they identified two examples where TLS had been reported to be absent: (i) amorphous silicon; (ii) low-density amorphous water.

Let us begin with the boson peak. From our experiments in amber, it is clear that this vibrational excess over the Debye level persists in such a hyperaged glass. Notice that its position does not vary with rejuvenation, though a modest increase of its height is observed following the increase of the elastic Debye level. In addition, a strong boson peak in C_p/T^3 had already been observed by us in (20 million years old) Dominican amber [10], though apparent residual curing or repolymerization, occurring around the glass transition temperature when rejuvenating those amber samples, hindered a reliable quantitative investigation. Although some authors have tried to correlate the boson peak feature in glasses [38], and even in crystals [39], with transformations of the elastic continuum only, such a Debye-scaling rule is not hold quantitatively in our case. The height of the C_p/T^3 boson peak in the hyperaged amber has decreased a 22% from the standard rejuvenated glass, whereas a Debye scaling [38] ($\propto \omega_D^{-3}$, with ω_D being the Debye frequency) would predict only a 7.4% reduction. Unfortunately, a similar discussion on the boson peak in ultrastable glasses of indomethacin is not possible since this feature is hardly seen in the specific-heat curves of this glass.

Nevertheless, the best fingerprint of the universal glassy anomalies is surely the density of TLS, measured from the corresponding quasilinear contribution to the specific heat, since the influence of Debye-like lattice vibrations becomes less and less important below 1 K. In this respect, our experimental results are conclusive: pristine, partially-rejuvenated and fully-rejuvenated amber glasses have the same specific heat below 1 K, within experimental error. Therefore, the boson peak and, especially, the tunneling TLS are robust and intrinsic properties of glasses which remain “fossilized” in 110-million-year stabilized glasses of amber. After this finding, our later results in ultrastable glasses of indomethacin were quite unexpected. As clearly demonstrated in Fig. 3 and Table 2, these USG exhibited a full suppression (within experimental error) of the TLS contribution to the specific heat, whereas similar glasses of the same substance lacking such ultrastability exhibited a typical contribution. Without the experiments on amber, one would be tempted to ascribe the found suppression of

the TLS in ultrastable glasses of IMC to the extraordinary stability (either thermodynamic or structural) of these particular glasses, and its corresponding large reduction in enthalpy or entropy, in the line of the “perfect glasses” mentioned above.

An alternative approach is the Random First Order Theory (RFOT) that explains the “universality” of TLS behavior at low temperature by the universality of the dynamical correlation length at T_g [40,41]. As such RFOT predicts that ultrastable glasses [42] should have a diminished density of two level systems. With the argument about the faster relaxation at glass surfaces that allows the correlation length to grow, the expected reduction in TLS should be roughly by a factor of between 4 and 8 [43]. This would go in the line of our experiments, though a full suppression is not explained.

Rather, we believe that the reason should be sought in some particularities of the ultrastable glass of indomethacin. In fact, some glasses obtained by physical vapor deposition show evidence of molecular anisotropy which is partly due to the growth method of thin films from the vapor phase. In particular, ultrastable IMC glasses exhibit an extra, low- q , peak in wide-angle x-ray scattering (WAXS) spectra [44] and birefringence in ellipsometric measurements [45]. In our experiments [9] we have shown that the low- q peak appears indeed in the WAXS pattern of our vapor-deposited ultrastable glass, whereas it is absent in the conventionally prepared glass. The presence of this peak for the ultrastable glass should be related to some sort of molecular order along the growth direction, perpendicular to the substrate, as clearly revealed in the in-plane/out-of plane diffraction experiments [9]. This orientation may be enabled by the high mobility of the indomethacin molecules when they impinge the substrate surface from the vapor [44]. The layered and anisotropic character of the USG of IMC could hence be the key of the observed behavior.

As mentioned in the Introduction, it has been stressed [6,7] that, in addition to the unexplained universality of the TM fitting parameters, the model in its original form neglects the fact that as a result of interaction with the strain (phonon) field, the tunneling TLS must acquire a mutual interaction. It can be shown [6,7] that the effective interaction between two TLS separated by a distance r is dipolar elastic and the interaction strength goes as $\sim g/r^3$, with $g = \gamma^2/\rho v^2$, where γ is the TLS-phonon coupling constant, ρ is the mass density and v is the sound velocity of a given substance. An ensemble of independent, noninteracting TLS would not be possible nor could justify the observed *quantitative* universality. Instead, the observed astonishing universality could emerge as the general result of some renormalization process of (almost) any ensemble of defects or manybody energy levels and stress matrix elements, interacting through the usual bath of thermal phonons, implying the existence of some crossover length

scale r_0 . Therefore, we think that the picture of a spherical volume of size r_0^3 comprising an isotropic random distribution of structural defects (TLS) embedded in a 3D vibrational lattice, allowing the interaction between resonant defects via the acoustic-phonon bath, may fail in the case of these layered and anisotropic ultrastable glasses of IMC. We suggest that a possible interpretation of the found suppression of TLS in ultrastable IMC thin-film glasses grown at $0.85 T_g$ could then be related to the modification of the molecular interaction in vapor-deposited USG films, through a decrease of free hydrogen bonds and an enhancement of π - π interactions between chlorophenyl rings. Further, water absorption seems to take place by occupying free sites of the IMC glass where water can hydrogen bond. Thus, without modifying the intrinsic structure of the layer, absorbed water molecules are able to bridge IMC molecules through hydrogen bonds, so feeding the interconnection of the dynamical network, and hence recovering the *interacting* TLS excitations, as we indeed observe in the “degraded” USG sample. Therefore, the found suppression of the two-level-systems would not be related to the extraordinary stability of the glass, but rather to the particular molecular arrangement ruled by the deposition conditions in this ultrastable glass.

Finally, highly-stable “ideal glasses” can be associated in our view with a negligible excess in *configurational* entropy, whereas non-crystalline solids lacking low-energy excitations (TLS, boson peak...) could be associated with a low vibrational entropy. Both features may be related sometimes, but they are not automatically connected, as the case of hyperaged amber shows.

5. Conclusions

To the best of our knowledge, no study had been performed up to date to investigate the possible effects that the dramatic increase in thermodynamic and kinetic stability of unique and selected kinds of glass could have on the universal low-temperature anomalies of glasses.

In the discussed experiments, we have studied two different kinds of extremely stabilized glasses, ideally approaching the “ideal glass” state with zero configurational entropy. Our experiments on hyperaged glasses of amber undoubtedly demonstrate that the low-temperature “anomalous” properties of glasses (TLS and the boson peak) persist essentially unchanged in ideal-like glasses, subjected to a dramatic thermodynamic and kinetic stabilization. Therefore, they are robust and intrinsic properties of glasses. In contrast, tunneling TLS unexpectedly disappear in ultrastable glasses of IMC, what we attribute to its very anisotropic and layered character. We speculate that it may lend support to the arguments by Leggett and others [6,7] which have claimed against the standard TM assuming independent, non-interacting TLS. Similar experiments in

nonlayered ultrastable glasses would be most interesting to confirm this interpretation.

Acknowledgments

The Laboratorio de Bajas Temperaturas (UAM) is an associated unit with the ICMM-CSIC. This work was financially supported by the Spanish MINECO, under FIS2011-23488, MAT2012-37276-C03-01 and MAT2010-15202 projects.

1. R.C. Zeller and R.O. Pohl, *Phys. Rev. B* **4**, 2029 (1971).
2. *Amorphous Solids: Low Temperature Properties*, W.A. Phillips (ed.), Springer-Verlag, Berlin, Heidelberg (1981).
3. R. Zorn, *Physics* **4**, 44 (2011), and references therein.
4. W.A. Phillips, *J. Low Temp. Phys.* **7**, 351 (1972).
5. P.W. Anderson, B.I. Halperin, and C.M. Varma, *Philos. Mag.* **25**, 1 (1972).
6. C.C. Yu and A.J. Leggett, *Comments Cond. Mat. Phys.* **14**, 231 (1988).
7. A.L. Burin, D. Natelson, D.D. Osheroff, and Y. Kagan, in: *Tunnelling Systems in Amorphous and Crystalline Solids*, P. Esquinazi (ed.), Springer, Berlin (1998), Chap. 3.
8. T. Pérez-Castañeda, R.J. Jiménez-Riobóo, and M.A. Ramos, *Phys. Rev. Lett.* **112**, 165901 (2014).
9. T. Pérez-Castañeda, C. Rodríguez-Tinoco, J. Rodríguez-Viejo, and M.A. Ramos, *PNAS* **111**, 11275 (2014).
10. T. Pérez-Castañeda, R.J. Jiménez-Riobóo, and M.A. Ramos, *J. Phys.: Condens. Matter* **25**, 295402 (2013).
11. S.F. Swallen, K.L. Kearns, M.K. Mapes, Y.S. Kim, R.J. McMahon, M.D. Ediger, T. Wu, L. Yu, and S. Satija, *Science* **315**, 353 (2007).
12. K.L. Kearns, S.F. Swallen, M.D. Ediger, T. Wu, and L. Yu, *J. Chem. Phys.* **127**, 154702 (2007).
13. E. León-Gutiérrez, A. Sepúlveda, G. García, M.T. Clavaguera-Mora, and J. Rodríguez-Viejo, *Phys. Chem. Chem. Phys.* **12**, 14693 (2010).
14. E. León-Gutiérrez, G. García, A.F. Lopeandía, M.T. Clavaguera-Mora, and J. Rodríguez-Viejo, *J. Phys. Chem. Lett.* **1**, 341 (2010).
15. S.L. Ramos, M. Oguni, K. Ishii, and H. Nakayama, *J. Phys. Chem. B* **115**, 14327 (2011).
16. M.D. Ediger and P. Harrowell, *J. Chem. Phys.* **137**, 080901 (2012).
17. F.H. Stillinger, *Science* **267**, 1935 (1995).
18. P.G. Debenedetti and F.H. Stillinger, *Nature* **410**, 259 (2001).
19. K.L. Kearns, S.F. Swallen, M.D. Ediger, T. Wu, Y. Sun, and L. Yu, *J. Phys. Chem. B* **112**, 4934 (2008).
20. C. Menor-Salván, M. Najarro, F. Velasco, I. Rosales, F. Tornos, and B.R.T. Simoneit, *Organic Geochemistry* **41**, 1089 (2010).
21. J.K. Krüger, J. Baller, T. Britz, A. le Coutre, R. Peter, R. Bactavatchalou, and J. Schreiber, *Phys. Rev. B* **66**, 012206 (2002).

22. E. Pérez-Enciso and M.A. Ramos, *Thermochimica Acta* **461**, 50 (2007).
23. A. Sepúlveda, E. León-Gutiérrez, M. González-Silveira, C. Rodríguez-Tinoco, M.T. Clavaguera-Mora, and J. Rodríguez-Viejo, *Phys. Rev. Lett.* **107**, 025901 (2011).
24. *Relaxation in Viscous Liquids and Glasses*, S. Brawer (ed), American Ceramic Society, Columbus (1985).
25. A.P. Sokolov, E. Rössler, A. Kisluk, and D. Quitmann, *Phys. Rev. Lett.* **71**, 2062 (1993).
26. R. Calemczuk, R. Lagnier, and E. Bonjour, *J. Non-Cryst. Solids* **34**, 149 (1979).
27. H. v. Löhneysen, H. Rüsing, and W. Sander, *Z. Phys. B* **60**, 323 (1985).
28. N. Ahmad, K. Hutt, and W.A. Phillips, *J. Phys. C* **19**, 3765 (1986).
29. S.L. Isakov, S.N. Ishmaev, V.K. Malinovsky, V.N. Novikov, P.P. Parshin, S.N. Popov, A.P. Sokolov, and M.G. Zemlyanov, *Physica A* **201**, 386 (1993).
30. E. Pérez-Enciso, M.A. Ramos, and S. Vieira, *Phys. Rev. B* **56**, 32 (1997); M.A. Ramos, J.A. Moreno, S. Vieira, C. Prieto, and J.F. Fernández, *J. Non-Cryst. Solids* **221**, 170 (1997).
31. R. Zorn and B. Frick, *J. Chem. Phys.* **108**, 3327 (1998).
32. E. Duval, L. Saviot, L. David, S. Etienne, and J.F. Jal, *Europhys. Lett.* **63**, 778 (2003).
33. X. Liu, B.E. White, Jr., R.O. Pohl, E. Iwanizcko, K.M. Jones, A.H. Mahan, B.N. Nelson, R.S. Crandall, and S. Veprek, *Phys. Rev. Lett.* **78**, 4418 (1997).
34. B.L. Zink, R. Pietri, and F. Hellman, *Phys. Rev. Lett.* **96**, 055902 (2006).
35. D.R. Queen, X. Liu, J. Karel, T.H. Metcalf, and F. Hellman, *Phys. Rev. Lett.* **110**, 135901 (2013).
36. N.I. Agladze and A.J. Sievers, *Phys. Rev. Lett.* **80**, 4209 (1998).
37. C.A. Angell, C.T. Moynihan, and M. Hemmati, *J. Non-Cryst. Solids* **274**, 319 (2000).
38. A. Monaco, A.I. Chumakov, Y.-Z. Yue, G. Monaco, L. Comez, D. Fioretto, W.A. Crichton, and R. Ruffer, *Phys. Rev. Lett.* **96**, 205502 (2006).
39. A.I. Chumakov, G. Monaco, A. Fontana, A. Bosak, R.P. Hermann, D. Bessas, B. Wehinger, W. A. Crichton, M. Krisch, R. Ruffer, G. Baldi, G. Carini Jr., G. Carini, G. D'Angelo, E. Gilioli, G. Tripodo, M. Zanatta, B. Winkler, V. Milman, K. Refson, M.T. Dove, N. Dubrovinskaia, L. Dubrovinsky, R. Keding, and Y.Z. Yue, *Phys. Rev. Lett.* **112**, 025502 (2014).
40. V. Lubchenko and P.G. Wolynes, *Phys. Rev. Lett.* **87**, 195901 (2001).
41. V. Lubchenko and P.G. Wolynes, in: *Adv. Chem. Phys.*, S.A. Rice (ed.), Wiley (2007), Vol. 136, p. 95.
42. J.D. Stevenson and P.G. Wolynes, *J. Chem. Phys.* **129**, 234514 (2008).
43. P.G. Wolynes (private communication).
44. K. Dawson, L. Zhu, L.A. Yu, and M.D. Ediger, *J. Phys. Chem. B* **115**, 455 (2011).
45. S.S. Dalal and M.D. Ediger, *J. Phys. Chem. Lett.* **3**, 1229 (2012).